

Automatic Hardware Pragma Insertion in High-Level Synthesis: A Non-Linear Programming Approach

Stéphane Pouget
pouget@cs.ucla.edu

University of California, Los Angeles

Louis-Noël Pouchet
pouchet@colostate.edu

Colorado State University

Jason Cong
cong@cs.ucla.edu

University of California, Los Angeles

ABSTRACT

High-Level Synthesis enables the rapid prototyping of hardware accelerators, by combining a high-level description of the functional behavior of a kernel with a set of micro-architecture optimizations as inputs. Such pragmas may describe the pipelining and replication of units, or even higher level transformations for HLS such as automatic data caching using the AMD/Xilinx Merlin compiler. Selecting the best combination of pragmas, even within a restricted set, remains particularly challenging and the typical state-of-practice uses design-space exploration to navigate this space. But due to the highly irregular performance distribution of pragma configurations, typical DSE approaches are either extremely time consuming, or operating on a severely restricted search space.

In this work we propose a framework to automatically insert HLS pragmas in regular loop-based programs, supporting pipelining, unit replication (coarse- and fine-grain), and data caching. We develop a simple analytical performance and resource model as a function of the input program properties and pragmas inserted. We prove this model provides a lower bound on the actual performance for any possible configuration. We then encode this model as a Non-Linear Program, by making the pragma configuration as unknowns of the system, which is computed optimally by solving this NLP. This approach can also be used during DSE, to quickly prune points with a (possibly partial) pragma configuration, employing this latency lower bound property. We extensively evaluate our end-to-end fully implemented system, showing it can effectively manipulate spaces of billions of designs in seconds to minutes for the kernels evaluated.

KEYWORDS

HLS, FPGA, Non-Linear Programming, Program Optimization

1 INTRODUCTION

High-level synthesis (HLS) [5, 36] compilers [13, 18, 24, 32] and source-to-source compiler for HLS [12, 14, 15, 31, 33, 34] can reduce development time while delivering a good performance for the designs. However, achieving a satisfactory Quality of Results (QoR) often requires design-space exploration (DSE). This is because the design space, including which pragmas to insert and where, can not only contain millions of points, but typically does not present characteristics suitable for fast analytical exploration, such as convexity and regularity. Although the existing DSE methods [25, 26, 30] can find designs with a good QoR, it comes at a high computation cost: for example hundreds, of designs may be concretely instantiated using HLS to compute its estimated QoR during exploration [26].

Our main objective is to provide a system to automatically insert a set of hardware pragmas for HLS that delivers a good QoR but significantly reduces the search time needed to obtain the final design.

To address this challenge, we propose NLP-DSE, a framework built on top of the AMD/Xilinx Merlin source-to-source compiler [31]. This framework automatically inserts pragmas for unrolling/parallelization, pipelining, tiling and data caching for linear programs prior to HLS. These Merlin pragmas can also be inserted using a DSE approach, such as AutoDSE [26], which we utilize as reference for our evaluations. However, in contrast to AutoDSE [26], we develop a hybrid analytical approach combined with a lightweight DSE, reducing the number of designs explored while preserving, and often even improving, the final QoR of designs produced.

To this end, we create a novel Non-Linear Programming approach to automatically insert pragmas in an existing program. We develop an analytical model combining latency and resources, targeting regular loop-based kernels [20], that is parameterized by the pragma configuration. We can then designate the pragma configuration as the unknowns of this model, solving it by NLP to obtain the set of pragmas that minimizes latency. An important design principle of our approach is to ensure that the latency computed is a *lower bound on the achievable latency for a given pragma configuration*. This enables efficient pruning during DSE: any design predicted to have a latency lower bound higher than the best latency obtained through exploration so far is necessarily slower and does not need exploration. To overcome the fact that optimizing compilers, and the overall HLS toolchain underneath, may not apply optimizations as expected (e.g., due to insufficient resources, or limitations of the compiler’s implementation), we develop a lightweight NLP-based DSE approach, exploring parts of the design space with different types and amounts of hardware parallelisms and array partitioning factors. We make the following contributions:

- We produce an analytical performance and resource model specifically built for AMD/Xilinx Vitis and Merlin compilers, which is amenable to optimization via non-linear programming.
- We prove our model is a lower bound on the final latency of the design, under reasonable hypothesis. This enables fast pruning of the design space, ensuring pruned designs have higher latency.
- We develop a NLP-based DSE approach exploiting this model, targeting regular loop-based kernels, which can significantly outperform DSE-based search approaches such as AutoDSE, delivering equal or better QoR in a significantly less search time.
- We implement NLP-DSE as an end-to-end fully automated system and use it to conduct extensive evaluation on 47 benchmarks including kernels from linear algebra, image processing, physics simulation, graph analytics, datamining, etc. [20]. Our results show the ability of our approach to find in most cases a better QoR than AutoDSE, in significantly less time.

The paper is organized as follows. Section 2 motivates our approach and solution proposed. Section 3 presents our analytical performance and resource model. Section 4 delves into proving it

is a lower bound on the final QoR. In Section 5, we introduce a non-linear formulation based on this model to automatically find pragma configurations by NLP optimization. Section 6 presents our lightweight DSE approach. Finally, Sections 7 and 9 are devoted to evaluating our method validating the effectiveness of our approach and presenting related work, before concluding.

2 BACKGROUND AND MOTIVATION

The main objective of this work is to automatically optimize FPGA designs using HLS [5, 36]. HLS has made FPGA usage more accessible, and many projects are looking to further democratize this field by automating optimizations [10, 12, 14, 26, 33] such as the AMD/Xilinx Merlin Compiler ([3, 4, 31]).

In particular, Merlin was developed to improve the performance and reduce the development time of HLS-based designs. To achieve this goal, it automatically generates data transfers between off-chip and on-chip memory and inserts important Vitis pragmas, such as for array partitioning. Merlin includes hardware directives pragmas such as `ACCEL parallel <factor=x>`, which creates x parallel instances, and Merlin restructures the code accordingly if the loop nest has more than x iterations. This pragma can be used for fine-grained and coarse-grained parallelization. There are also the pragmas `ACCEL pipeline <II=y>` for pipelining, and `ACCEL tile <factor=z>` for strip-mining a loop by z , enabling Merlin to insert other pragmas such as data caching in a loop with smaller trip count, matching the on-chip resources available and reducing off-chip communications. Merlin’s `ACCEL cache <array=a>` directive transfers all required elements of array a from off-chip to on-chip to perform computations within the specified sub-region.

2.1 DSE for Pragma Insertion

Tools such as AutoDSE [26] and GNN-DSE [25] rely on Merlin and perform DSE to find which pragmas to insert and where.

Although Merlin further raises the level of abstraction and easiness to implement complex transformations such as data caching and various types of hardware replication and hence reduces the space of configurations, the space of pragmas and their parameter values is still large: as shown later in Sec. 7, this space quickly reaches billions of feasible designs even for kernels containing only a handful of loops and statements.

Furthermore, to avoid accuracy limitations of analytical performance models, DSE approaches exploring such space typically rely on partially generating the design, at least via HLS, and utilizing the QoR report as the performance estimate for a design. HLS time for highly optimized designs combining various Merlin pragmas (e.g., parallelism and caching) can quickly reach several hours per design, making the search process particularly time-consuming. One may restrict the space of pragmas considered, and especially their parameter range, to reduce search time [26]. However this comes at the expense of the potentially improved performance that can be reached by considering the complete parameter space.

Yet such DSE remains the state-of-practice approach to deliver high-quality designs, we illustrate its performance merits with three sample benchmarks from linear algebra: *GEMM*, the dense

generalized matrix-multiply, *2mm*, which computes the matrix product $D = A * B * C$, and *Gramschmidt*, which computes the Gram-Schmidt process for QR decomposition. Table 1 below displays the performance (in GigaFlop/s, GF/s) of the original program from PolyBench/C using the Medium dataset size and Large for Gramschmidt, without any pragmas, and optimized by Merlin and the final performance achieved by running AutoDSE to insert Merlin pragmas, given a time budget of 20 hours and a timeout of 3 hours per HLS run. DSE time is reported in minutes.

	2mm		Gemm		Gramsch.	
	GF/s	Time	GF/s	Time	GF/s	Time
Original	0.10	N/A	0.07	N/A	0.14	N/A
AutoDSE	0.41	1,870	68.91	1,345	0.95	819
NLP-DSE	117.48	70	105.18	185	2.34	420

Table 1: Result of AutoDSE

This framework utilizes the HLS compilers as a black box used to select configurations that minimize the objective function. The tool is agnostic of the input program shape and if it detects that Merlin did not apply the pragmas as expected it allows the DSE to prune the design after Merlin has generated the HLS-C code.

By analyzing the space explored by the DSE for these three examples, valuable hints can be observed to improve the method. For 2mm, the fastest design found by AutoDSE is mainly optimized for a single loop body. When AutoDSE tries to optimize the second loop body, it favors the unroll factors to the power of two for the innermost loop and goes directly to the outermost loop. This does not improve performance or create configurations which are pruned. The fact that it does not try the other unrolls factors for the innermost loop before optimizing the other pragmas creates a loss of performance. For Gemm Medium and Gramschmidt Large, the DSE makes it possible to find designs with a good QoR. However the DSE wastes much time exploring too large unroll factors, which generates ponderously long synthesis times without giving any result as the HLS timeout is reached. The time spent increasing the unroll factor for certain pragmas without result does not allow the unroll factor of other pragmas to be increased, which results in missed performance.

2.2 Overview of NLP-DSE

Our primary objective is to efficiently achieve high-quality designs within a limited compilation time budget. To accomplish this we develop a DSE based on a cost model which can find the *theoretical* optimal configuration in a few seconds/minutes, thanks to its implementation as a Non-Linear Programming (NLP) problem which is then solved using BARON [27]. Note, however, the *in-practice* configuration that achieves the best performance may be different: our NLP is unable to model the complexity of the downstream toolchain and issues of resource usage/sharing, actual implementation of the pragmas by Merlin and Vitis, and simple performance bugs in these optimizing compilers may imply a theoretically best design is not implemented as such, making a design space exploration approach still required to achieve a good performance. We have therefore set up a DSE which allows the framework to explore different spaces of parallelism as well as different configuration spaces by constraining the level of parallelism. Our model is presented in Sec. 3, and we

prove it is a performance lower bound in Sec. 4, an important feature to be able to prune designs during the search without the risk of losing performance. The associated NLP formulation is given in Sec. 5.

To make our approach feasible, and in particular maintain a sufficient level of accuracy in the analytical models, we target regular, loop-based computations, that is *affine programs* [7]. Such programs have a static control-flow, that is every operation executed, and a branch taken at run-time, can be exactly modeled at the compile-time using polyhedral structures [9]. This restriction improves accuracy of loop-based analytical model by providing them with exact information about the loop trip counts and dependencies.

It is important to note that our DSE process, presented in Sec. 6, fundamentally differs from AutoDSE. We first evaluate configurations that have the lowest theoretical latency, and hence typically a high level of parallelism. However AutoDSE starts from a configuration with no pragmas, which is typically feasible in terms of resource usage, and progressively increases the pragmas until resources are exceeded. Instead our NLP-DSE begins with a design featuring the maximum achievable parallelism, and then gradually reduces the level of parallelism. We illustrate this with Table 1 with the final performance and time-to-solution achieved by NLP-DSE.

As presented in Sec. 7, compared to AutoDSE, our framework locates designs with similar or higher throughput for 46 out of 47 benchmarks evaluated, with a performance improvement of 5.69x and 17.24x on average in terms of the DSE time and design throughput respectively. Only 1 design having a 7% lower throughput. In all 47 benchmarks, the time-to-solution of NLP-DSE is significantly less than AutoDSE, up to 30x faster.

3 MODELING PROGRAMS AND THEIR PRAGMAS

We now present our analytical performance model. We assume the input programs are polyhedral programs [9, 11], and therefore exact loop trip counts can be computed by static analysis, similarly for all data dependencies.

3.1 Program Representation

We represent programs using a summary of their Abstract syntax tree (AST), with sufficient information to estimate latency and resource consumption by analytical modeling. Intuitively, we can build a constructor-style description of the summary AST, and then directly instantiate the complete formula for estimating e.g., latency, based on loop properties. We first introduce this representation before proving how to compute a latency lower bound with it.

We employ the code below as a running example with the pragma above the loops as AMD/Xilinx Merlin and OpenMP. For presentation simplicity, we assume each loop iterator in the program region has been renamed to a unique name, so that we can uniquely identify loops in the code by their iterator name.

```

1 <some-pragmas-for-loop-i>
2 for (i = lbi; i <= ubi; i++) {
3   <some-pragmas-for-loop-j1>
4   for (j1 = lbj1(i); j1 <= ubj1(i); j1++) S1(i, j1);
5   <some-pragmas-for-loop-j2>
6   for (j2=lbj2(i); j2<=ubj2(i); j2++){S2(i, j2); S3(i, j2);}}
```

The summary AST for this loop is simply built by creating one node per for loop and one per statement S_x , the body of a loop is made of loops and/or statements, and their nodes are children of said loop in the tree, listed in their syntactic order. For example, above, utilizing a constructor notation, it gives: $Loop_i(Loop_{j1}(S1), Loop_{j2}(S2, S3))$. Then, a simple rewrites of this tree using loop properties and composition operators will lead to the proposed analytical model, as outlined below.

We now describe the loop properties we associate to each loop. We consider combinations of the following pragmas, based on Merlin’s optimizations, for the loop with iterator i : `#pragma ACCEL parallel <factor=ufi>`, `#pragma ACCEL pipeline <II=IIi>`, `#pragma ACCEL tile` and `#pragma ACCEL cache <variable=a>`.

We therefore associate to each loop i in the program a *property vector* that informs about the optimizations to be considered. We define \vec{PV}_i as follows: $\vec{PV}_i :< ispipelined_i, II_i, ufi, tile_i, TC_i^{min}, TC_i^{max} >$ where we have: $ispipelined_i = 1$ if the loop is pipelined, 0 otherwise; II_i is the initiation interval, set to 1 by default; ufi is the parallelism/unroll factor, set to 1 by default (no `#pragma ACCEL parallel` pragma) and set to TC_i^{max} if `parallel` is defined without a factor ufi specified. $tile_i$ is the TC of the innermost loop after strip mining. TC_i^{min} is the minimal trip count of loop i , for any of its execution in the program. We also compute the maximal trip count over all executions. These values are computed using polyhedral analysis on the loops [21]. The pragma cache transfers above the loop i the data needed for the computation of this loop nest for the array a .

This vector is built by syntactic analysis on the program, where the default value $PV_i :< 0, 1, 1, 1, TC_i^{min}, TC_i^{max} >$ is used for a loop without any pragma. Once all loops have been annotated by their \vec{PV} properties, subsequent treatment can be implemented to mirror the optimizations implemented by the back-end tool.

Modeling Vitis optimizations AMD/Xilinx Vitis will apply several optimizations automatically, such as auto-pipeline and auto-loop-flatten, some other optimizations when the user gives a compilation option such as tree reduction.

Only a loop with a constant TC , i.e., $TC_{max} = TC_{min}$ can be unrolled. The unroll pragma options allow to specify the unrolling factor, ufi . When the factor is not specified, it implies that the factor is equal to the TC of the loop. When a loop is pipelined, all innermost loops are automatically fully unrolled. Hence, we also propagate unrolling information, e.g., to mark a full loop nest for full unrolling if an outer loop is marked with `#pragma ACCEL pipeline`. The pipeline pragma options allow to specify the objective II the user wants to achieve. When II is not specified, it is automatically set to 1. In addition, Vitis will auto-pipeline with a target II of 1 the innermost loop which are not fully unrolled for each nested loop.

Within Vitis, users can enable optimizations like logarithmic time reduction through tree reduction. This optimization choice will be a global option within our model, applicable across the entire model rather than being limited to a specific loop.

Modeling Merlin optimizations Finally, Merlin will also add automatic optimizations. It will explicitly strip-mine a loop when it is partially unrolled with the innermost loop having a TC equal to the factor and the unrolled pragma applied to that loop. Similarly to Vitis, Merlin will auto-pipeline. Merlin also applies a program transformation for certain pragmas. When there are two perfectly

nested and partially unrolled loops, Merlin swaps the two loops strip-mined (if legal), unrolled innermost and flatten and pipeline the two outermost loops. Further, Merlin will automatically transfer the data from off-chip to on-chip and cache on-chip with packing, with a maximum packing of 512 bits for our FPGA while computing if the footprint of the data fit on-chip by static analysis. The pragma tile allows Merlin to strip mine a loop and give the compiler the opportunity to transfer less/more data while respecting resource constraints. For our model we suppose an optimistic data transfer i.e., all memory transfers are done with a packing of 512 bits and each data are transferred once (perfect data reuse).

Consequently, the set of possible $\vec{P}\vec{V}_i$ vectors are adjusted by analyzing the input code, and modifying their initial value, possibly further constraining the set of possible $\vec{P}\vec{V}_i$ based on which program transformation will be performed, as described above. Overall, the $\vec{P}\vec{V}_i$ vectors, along with the summarized AST, contain sufficient information to capture several source-to-source transformations performed by the Merlin compiler for coarse- and fine-grain parallelization, and reason on the likeliness of the optimization to succeed at HLS time (e.g., capturing loops with non-constant trip count).

4 THEORETICAL LATENCY AND RESOURCE MODELING

We now outline key elements of our analytical performance model, and the associated proofs this model computes a lower bound on latency under resource constraints. Full proofs cover several pages, and are available in the Appendix : we limit below to summarizing the hypothesis and overall proof approach.

4.1 Analytical Model Template

We take as input the summary AST of the program in constructor form, and the set of $\vec{P}\vec{V}_i$ vectors for each loop, as defined in Sec. 3.1. Returning to our example in Sec. 3.1, this summary AST, capturing the loop structure and all statements, is $Loop_i(Loop_{j_1}(S1), Loop_{j_2}(S2, S3))$

Let $I_i^{\vec{P}\vec{V}_i}(X)$ be an operator that computes the latency of a region of a code represented by X , where X is composed of loops and/or statements. This function is computed as follows: $I_i^{\vec{P}\vec{V}_i}(X) = \lfloor II_i * (TC_i^{avg} / u_{fi} - pip_i) \rfloor \odot X$ where \odot is $+$ if the loop i is pipelined ($pip_i = 1$), \times otherwise. Let $C_i^{\vec{P}\vec{V}_i}(X_1, \dots, X_n)$ the operators which composed the region, defined as follows: $C_i^{\vec{P}\vec{V}_i}(X_1, \dots, X_n)$ is $\max_{i=1}^n(X_i)$ if there is no dependency (WaR, RaW, WaW) between the statements of the regions and $\sum_{i=1}^n X_i$ between the statements which have at least one dependency. Finally, $SL_i^{\vec{P}\vec{V}_i}(\vec{S}_k)$ denotes a region of straight-line code (e.g., an inner-loop body). Intuitively, SL will represent a lower bound on the latency of a code block such that, by the composition across all loops as per the template formula, the result remains a lower bound on the full program latency.

We build the analytical formula template by simple substitution of the operators in the summary AST by the following operators: (1) for every $Loop_i(\vec{X})$, replace it by $I_i^{\vec{P}\vec{V}_i}(\vec{X})$; (2) for every list \vec{I} containing the $I_i^{\vec{P}\vec{V}_i}(\vec{X})$ of the step 1, replace it by $C_i^{\vec{P}\vec{V}_i}(\vec{I})$; and (3)

replace statement lists inside loop i \vec{S}_x by $SL_i^{\vec{P}\vec{V}_i}(\vec{S}_x)$. That is for our example, we simply rewrite: $Loop_i(Loop_{j_1}(S1), Loop_{j_2}(S2, S3))$ into the following formula:

$$I_i^{\vec{P}\vec{V}_i}(C_i^{\vec{P}\vec{V}_i}(I_{j_1}^{\vec{P}\vec{V}_{j_1}}(SL_{j_1}^{\vec{P}\vec{V}_{j_1}}(S1)), I_{j_2}^{\vec{P}\vec{V}_{j_2}}(SL_{j_2}^{\vec{P}\vec{V}_{j_2}}(S2, S3))))$$

4.2 Restrictions and Applicability

Our objective is to formulate a lower bound on the latency of a program, after HLS. We therefore include several restrictions:

- The input program is a pure polyhedral program [11], and its analysis (loop trip counts for every loop, all data dependencies [8]) is exact.
- No HLS optimization shall change the number of operations in the computation: strength reduction, common sub-expression elimination, etc., shall either first be performed in the input program before analysis, or not be performed by the HLS toolchain.
- The program does not contain "useless" operations. A typical case is when a value is overwritten before being utilized, e.g., $x = 42+51$; $x = 0$;
- We only model DSP and BRAM resources for the considered kernel, ignoring all other resources.
- We assume resources (DSP) sharing across different operations executing at the same cycle is not possible.

4.3 Latency Lower Bound

An important term is SL , a latency lower bound for a region of straight-line code. To maintain a lower bound on latency by composition, we operate on a representation of (parts of the) program which is both schedule-independent and storage-independent: the operation graph, or CDAG [6]. Indeed, a lower bound on this representation is necessarily valid under any schedule and storage eventually implemented and can be used to prove I/O lower bounds on programs [6] which is the directed acyclic graph with one node per operation in the code region, connecting all producer and consumer operations to build the operation graph. Then, we can easily compute the length of its critical path, which represents the minimal set of operations to execute serially.

Then, we can build a lower bound on the number of cycles a region L may require to execute, under fixed resources, by simply taking the maximum between the weighted critical path and the work to execute normalized by the resources available.

THEOREM 4.1 (LATENCY LOWER BOUND UNDER OPERATION RESOURCE CONSTRAINTS). *Given O the set of operation type and R_o a count of available resources of type $o \in O$, OG the operation graph, cp_L the critical path of OG , and $LO(o)$ the latency function for operation o , with $LO(o) \geq 1$. N_o^L denotes the number of operations of type o in L . We define $C_L = \sum_{n \in cp_L} LO(n)$ the critical path of L weighted by latency of its operations. The minimal latency of a region L is bounded by*

$$Lat_{R_o}^L \geq \max(C_L, \max_{o \in O} (\lceil N_o^L \times LO(o) / R_o \rceil))$$

This theorem provides the building block to our analysis: if reasoning on a straight-line code region, without any loop, then building the operation graph for this region and reasoning on its critical path is sufficient to provide a latency lower bound.

```

1 L1: for (i = 0; i < N; i++) S0: s[i] = 0;
2 L2: for (i = 0; i < M; i++) { S1: q[i] = 0;
3   L3: for (j = 0; j < N; j++) {
4     S2: s[j]+=r[i]*A[i][j]; S3: q[i]+=A[i][j]*p[j];}}

```

Listing 1: Big

For example in Lst. 1, if we consider the sub-loop body composed of loops L3 (fully unrolled) and the statements S2 and S3 as straight-line code regions, we can calculate the critical paths for S2 and S3 as follows: For S2, the critical path is given by: $cp_{S2} = \max(L(+) + L(*), N \times (DSP_+ + DSP_*)/R_o)$ with DSP_o the number of DSP for the operation o . For S3, the critical path is determined by: $cp_{S3} = \max(L(+) \times \log(N) + L(*), N \times (DSP_+ + DSP_*)/R_o)$, considering the possibility of a tree reduction. In this context, the critical path for the entire sub-loop body is the maximum of these two individual critical paths, expressed as $\max(cp_{S2}, cp_{S3})$.

We now need to integrate loops and enable composition of latency bounds.

Loop Unrolling Loop unrolling is an HLS optimization that aims to execute multiple iterations of a loop in parallel. Intuitively, for an unroll factor $UF \geq 1$, UF replications of the loop body will be instantiated. If $TC_l \bmod UF_l \neq 0$ then an epilogue code to execute the remaining $TC_l \bmod UF_l$ iterations is needed.

Unrolling can be viewed as a two-step transformation: first strip-mine the loop by the unroll factor, then consider the inner loop obtained to be fully-unrolled. The latency of the resulting sub-program is determined by how the outer-loop generated will be implemented. We assume without additional explicit information this unrolled loop will execute in a non-pipelined, non-parallel fashion. Note this bound requires to build the operation graph for the whole loop body. This is straightforward for inner loops and/or fully unrolled loop nests, but impractical if the loop body contains other loops. We therefore define a weaker, but more practical, bound that enables composition:

THEOREM 4.2 (MINIMAL LATENCY OF A PARTIALLY UNROLLED LOOP WITH FACTOR UF AND COMPLEX LOOP BODIES). *Given a loop l with trip count TC_l and loop body L , unroll factor $UF \leq TC$ and O the set of operation type. Given available resources R_o and latencies $L(o) \geq 1$ with $o \in O$. Then the minimal latency of l if executed in a non-pipelined fashion is bounded by:*

$$Lat_{R_o}^{l,S} \geq \lfloor TC/UF \rfloor * Lat_{R_o}^L$$

The intuition of the proof of Theorem 4.2 is that there cannot exist a shorter critical path in the operation graph of the unrolled loop nest than in the non-unrolled loop body, that is there is no useless operation. This is therefore essential to require the absence of useless operations in the program, as otherwise a shorter critical path may be exposed after loop unrolling, making this theorem incorrect.

Consider the scenario of loop $L0$ within Listing 1, which has been unrolled by a factor denoted as $UF \leq TC_{L0}$ where TC_{L0} is the trip count of $L0$. The latency for one iteration of $S0$ is denoted as $Lat_{R_o}^{S0} > 0$. In the absence of pipelining, the lower bound of the latency of this sub-loop body is: $\lfloor TC_{L0}/UF \rfloor \times Lat_{R_o}^{S0}$.

Loop pipelining Loop pipelining amounts to overlapping multiple iterations of the loop, so that the next iteration can start prior to the completion of the preceding one. The initiation interval (II)

measures in cycles the delay between the start of two consecutive iterations. It is easy to prove our formula template accurately integrates the latency of pipelined loops with the I operator. We compute the minimal II in function of the dependencies of the pipelined loop and the iteration latency of the operations of the statements during the NLP generation. Let $RecMII$ and $ResMII$ be the recurrence constraints and the resource constraints of the pipelined loop, respectively. We have $II \geq \max(ResMII, RecMII)$. $RecMII = \max_i \lceil \frac{delay(c_i)}{distance(c_i)} \rceil$ with $delay(c_i)$ the total latency in dependency cycle c_i and $distance(c_i)$ the total distance in dependency cycle c_i . We suppose that $ResMII = 1$, as we don't know how the resource will be used by the compiler. Hence, if the loop is a reduction loop then the $II \geq \frac{IL_{reduction}}{1}$ with $IL_{reduction}$ the iteration latency of the operation of reduction. For a kernel like $for(j = 0; j < N; j++) y[j] = y[j - 2] + 3$; the $II \geq \lceil \frac{IL}{2} \rceil$.

Program latency lower bound

We now focus on having the program latency lower bound, with resource constraints. This bound takes into account the limitations imposed by available resources, which can significantly affect the achievable performance. We assume here that the resources consumed are only consumed by the computing units and resource use by the computational unit of one operation can not be reused by the computational unit of another operation executing at the same time. We also assume that the compilers have implemented the pragma configuration given as input.

For DSPs we suppose we have a perfect reuse, i.e., that the computation units for the same operation can be reused as soon as the computation unit is not in use. Under-estimating the resources used is fundamental to proving the latency lower bound, as otherwise another design that consumes less resources than predicted may be feasible, itself possibly leading to a better latency. The lower bound of a kernel is therefore the lower bound of the configuration such that the minimal resource consumption is less than or equal to the resource available.

THEOREM 4.3 (LOWER BOUND OF THE KERNEL UNDER RESOURCE CONSTRAINT). *Given a loop body L , the set of statements S , O the set of operation type, N_o^s the number of operations $o \in O$ for the statements s , DSP_o the number of resources (DSPs) used for the operation $o \in O$, MCU_o^s the maximal computational unit the statement s can use in parallel and the configuration of pragma which is constituted of the vectors \vec{P}_i for each loop. The configuration of pragma, which has the minimal lower bound and which respect $R_{used}^{min} = \sum_o \max_{s \in S} (N_o^s \times DSP_o \times MCU_o^s) \leq R_o$, is the lower bound of the kernel.*

The intuition of the proof of the Theorem 4.3 is that R_{used}^{min} is the minimal resource that the kernel can use for the configuration of pragma. This implies that if the $R_{used}^{min} > R_o$ the configuration over-utilizes resources. Hence, the lowest lower bound which does not over-utilize the resource is the lower bound of the kernel.

5 NON-LINEAR FORMULATION FOR PRAGMA INSERTION

We now present the complete set of constraints and variables employed to encode the latency and resource model as a non-linear program. This section presents a modeling of section 4 in the practical case.

Let \mathcal{L} be the set of loops, \mathcal{A} the set of arrays, \mathcal{S} the set of statements and \mathcal{O}_s the operations of the statements s . In order to have an accurate model we distinguish for each statement the operation which can be done in parallel, i.e., does not have any loop-carried dependence, $\mathcal{O}_{s_{par}}$ and the reduction operations, i.e., associative/commutative operators to reduce one or more values into a single value, leading to loop-carried dependencies, $\mathcal{O}_{s_{red}}$.

Let \mathcal{P} be the set of different possible pipeline configurations. Let $\forall p \in \mathcal{P}$ define \mathcal{L}_{pip}^p the set of loops pipelined and $\forall l \in \mathcal{L}_{pip}^p$, $\mathcal{L}_{under_pip}^p$ the set of loops under a loop pipelined and $\mathcal{L}_{above_pip}^p$ the set of loops above the loop pipelined l . Let $\forall s \in \mathcal{S}$ define the set of nested loops which iterate the statement s , \mathcal{L}_s . $\forall a \in \mathcal{A}$ and for d a dimension of the array a , let C_{ad} be the set of loops which iterates the array a at the dimension d . $\forall l \in \mathcal{L}$, let designate d_l the maximum dependency distance of the loop l . And let II_s be the II of the loop pipelined for the statement s .

The II for each loop, the dependencies, the properties of the loops, the TC, the iteration latency of the parallel operations and the reduction operations and the number of DSPs per operation per statements are computed at compile time with PolyOpt-HLS [21] and used as constants in the NLP problem.

5.1 Variables

Variables in the formulation correspond to PV_l attributes. We consider the possibilities of pipelining (Eq. 3), unrolling (Eq. 1), and tiling (Eq. 2) for each loop. Additionally, we include the possibility of caching an array that is iterated over by the loop (Eq. 4).

5.2 Modeling Compiler Transformations

Now that we have defined our design space, we need to constrain the space by removing infeasible cases and those that do not comply with the rules of the compilers.

Pipeline Rules Vitis HLS unrolls all loops under the pipelined loop. This implies that all loop l under the pipelined loop must have $loop_l_UF == TC_l$ (Eq. 15). Considering this constraint, it is important to note that only one pipelined loop can exist per nested loop (Eq. 5). If multiple pipelined loops were present, the loops beneath the first pipelined loop would be unrolled instead.

Memory Transfer Rules Merlin automates the process of transferring data on-chip and applying array partitioning. The tool caches data on-chip and packs it in chunks of up to 512 bits, enabling efficient transfer speed. When the data is already present on-chip it can be reused provided that resource constraints are satisfied. The compiler caches on-chip the data only above the loop pipelined (Eq. 14).

Dependencies Loop-carried dependencies are managed using constraints (Eq 8). If a loop has a dependency distance of n , this means that if we unroll with an unroll factor $uf > n$ this is equivalent to unrolling the loop with a factor $uf = n$ because the statements corresponding to the iteration $\{uf + 1, \dots, n\}$ will be executed only after the first n statements are executed due to the dependency. Loop-independent data dependencies are managed at the objective function, as elaborated in Section 5.4.

Supplementary Rules In addition, we add the constraints for the maximum unrolling (Eq. 10), the divisibility of the problem size of the unroll factors (Eq. 6), the tile size (Eq. 7) and the maximum

array partitioning (Eq. 13). For this last, this corresponds to adding an upper bound to the product of the UF of all the loops which iterate the same array on different dimensions.

During our DSE, we can force the solution to be fine-grained. In this case we add a constraint where the loop above the loop pipelined has a UF of 1, i.e., for all loop l above the pipelined loop $loop_l_UF == 1$ (Eq. 9). We also constrain the resources, modeling their sharing optimistically. We consider the number of DSPs (Eq. 11) and on-chip memory (Eq. 12) used. As the consumption of DSPs can be difficult to estimate due to resource sharing we utilize an optimistic estimate, which considers a perfect reuse/sharing: as soon as a computation unit is free, its resource can be reused.

5.3 Constraints

$$\forall l \in \mathcal{L}, 1 \leq loop_l_UF \leq TC_l \quad (1)$$

$$\forall l \in \mathcal{L}, 1 \leq loop_l_tile \leq TC_l \quad (2)$$

$$\forall l \in \mathcal{L}, loop_l_pip \in \{0, 1\} \quad (3)$$

$$\forall l \in \mathcal{L}, \forall a \in \mathcal{A}, loop_l_cache_array_a \in \{0, 1\} \quad (4)$$

$$\forall s \in \mathcal{S}, \sum_{l \in \mathcal{L}_s} loop_l_pip \leq 1 \quad (5)$$

$$\forall l \in \mathcal{L}, loop_l_UF \% TC_l == 0 \quad (6)$$

$$\forall l \in \mathcal{L}, loop_l_tile \% TC_l == 0 \quad (7)$$

$$\forall l \in \mathcal{L}, \text{if } dd_l > 1, loop_l_UF \leq d_l \quad (8)$$

$$\forall l \in \mathcal{L}, \forall l' \in \mathcal{L}_{above_l}, loop_l_pip * loop_{l'}_UF \leq 1 \quad (9)$$

$$\forall s \in \mathcal{S}, \prod_{l \in \mathcal{L}_s} loop_l_UF \leq MAX_PARTITIONING \quad (10)$$

$$DSPs_used_{optimistic} = \sum_{op \in \{+, -, *, /\}} \max_{s \in \mathcal{S}} (DSP_{s_{op}} / II_s) \quad (11)$$

$$\begin{cases} \sum_{a \in \mathcal{A}} \sum_{l \in \mathcal{L}} loop_l_cache_array_a \\ \times footprint_array_a_loop_l \leq Mem \end{cases} \quad (12)$$

$$\begin{cases} \forall a \in \mathcal{A}, \forall (d, d') \in \mathbb{N}^2 \text{ with } d \neq d', \forall l \in C_{ad}, \forall l' \in C_{ad'}, \\ loop_l_UF \times loop_{l'}_UF \leq MAX_PARTITIONING \end{cases} \quad (13)$$

$$\begin{cases} \forall p \in \mathcal{P}, \forall l_p \in \mathcal{L}_{pip}^p, \forall l_{bp} \in \mathcal{L}_{under_pip}^p, \forall a \in \mathcal{A}, \\ loop_{l_{bp}}_cache_array_a == 0 \end{cases} \quad (14)$$

$$\begin{cases} \forall p \in \mathcal{P}, \forall l_p \in \mathcal{L}_{pip}^p, \forall l_{bp} \in \mathcal{L}_{under_pip}^p, \\ loop_{l_p} \times loop_{l_{bp}}_UF == loop_{l_p} \times TC_{l_{bp}} \end{cases} \quad (15)$$

5.4 Objective function

Lastly, we need to define the objective function (*obj_func*) that supports fine-grained and coarse-grained parallelism. Fine-grained parallelism involves duplicating a specific statement(s), while coarse-grained parallelism duplicates modules, including statements and loops. However, it may not always be feasible to achieve parallelism based on the characteristics of the loops and the level of parallelism required. Therefore, we distinguish between parallel and reduction loops. A parallel loop can be coarse and fine-grained unrolled, whereas a reduction loop can only be fine-grained unrolled with a tree reduction process that operates in logarithmic time.

As the pragmas cache are part of the space we compute the communication latency with these pragmas. If more than one array is transferred above the same loop we take the maximum as Merlin transferred them in parallel. To ensure these properties, we formulate the objective function for each pipeline configuration. The objective function uses the combined latencies of communication and computation. When using Merlin, communication and computation do not overlap, but communication tasks can overlap when they occur consecutively in the code at the same level. Consequently, for each loop, where two arrays are transferred consecutively within the loop, we calculate the sum of the maximum latencies for these transferred arrays (L_{mem}).

In every loop nest, there will invariably be a pipeline loop due to either user-inserted or compiler-inserted instructions (AMD/Xilinx Merlin and Vitis automatically insert the pragma pipeline if it is not done by the user or the previous compiler). Therefore, the objective function takes the following form: $TC_{ap} \times (IL + II \times (\frac{TC}{UF} - 1))$, where TC_{ap} includes the loops situated above the pipeline. Parallel loops above the pipeline can be coarse-grained parallelized. The iteration latency within the unrolled loop body is divided into either reduction operations or non-reduction operations, as reduction operations require logarithmic time for the reduction process. The variable IL encompasses the latencies of the statements found within the pipelined loop body. Independent statements can be executed in parallel and statements with dependencies are summed, as detailed in Section 4.1.

$$\begin{cases} TC_{ap} = \prod_{l \in \mathcal{L}^{par}} \frac{TC_l}{loop_l_{UF}} \times \prod_{l \in \mathcal{L}^{red}} TC_l \\ IL = IL_{par} + IL_{seq} \times \prod_{l \in \mathcal{L}^{red}} \frac{TC_l}{loop_l_{UF}} \times \log_2(loop_l_{UF}) \\ L_{mem} = \sum_{l \in \mathcal{L}} \max_{a \in \mathcal{A}} (loop_l_{cache_a} \times footprint_a_{loop_l}) \\ obj_func = TC_{ap} \times (IL + II \times (\frac{TC_{lp}}{loop_{lp}_{UF}} - 1)) + L_{mem} \end{cases}$$

5.5 Example

```

1 Loop0: for(i=0; i<2100; i++) S0:y[i] = 0;
2 Loop1: for(i=0; i<1900; i++) { S1:t[i] = 0;
3   Loop2: for(j=0; j<2100; j++) S2:t[i]+=A[i][j]*x[j];
4   Loop3: for(j=0; j<2100; j++) S3:y[j]+=A[i][j]*t[i];

```

Listing 2: Atax Large

We now employ the Atax kernel as an illustration. S_0 and S_3 do not have inter-iteration dependencies within their respective loops, namely $Loop_0$ and $Loop_3$. Therefore, it is possible to pipeline $Loop_0$ and $Loop_3$ with an $II \geq 1$. In other words, for all iterations within these loops, there are no dependencies on previous iterations within the same loop. $Loop_1$ and $Loop_2$ are reduction loops, and the reduction operations is an addition which has an IL of IL_+ cycles. So the $II \geq IL_+$. If $loop_1$ is pipelined, there is a dependency between S_1 , S_2 and S_3 . Between S_1 and S_2 the distance is 1, so we just add IL_{S_1} and IL_{S_2} . Between S_2 and S_3 the distance is $\log(N)$ so the final equation will be $IL_{S_1} + IL_{S_2} * \log(N) + IL_{S_3}$ for the loop body cycle. If statements can be run at the same time (i.e., there is no dependency) it is a max instead of an addition. If we encounter code like $for(j = 0; j < N; j++) y[j] = y[j - 2] + 3;$, a straightforward approach to handling this type of dependency is to impose a constraint such as $loop_l_{UF} \leq 2$, which is represented by

equation 8. In this case, due to dependencies an $UF > 2$ is similar to $UF = 2$.

6 DESIGN SPACE EXPLORATION

We now present our Design Space Exploration (DSE) approach. Our approach focuses on identifying designs with the most promising theoretical latency within the available design space. However, it may result in suboptimal designs if the selected pragmas are not applied during compilation. To address this potential issue and ensure high QoR, we conduct an additional exploration within a restricted subspace. Our DSE explores two additional parameters: the type of parallelism and the maximum array partitioning factor. Array partitioning is a technique commonly used in FPGA contexts to divide arrays or matrices into smaller sub-arrays, which can be stored in independent memory blocks known as Block RAMs (BRAMs). AMD/Xilinx HLS has a limit of 1,024 partitions per array. The array partitioning is calculated by taking the product of loops that iterate the same arrays on different dimensions (cf. Section 5). So constraining the maximal array partitioning also constrains the maximal UF . This NLP based DSE technique is presented in the Algorithm 1. The DSE starts without constraint on parallelism and array partitioning. Then we alternate constraints on parallelism while decreasing the maximum unrolling factor and array partitioning.

```

Data: kernel // without Pragma
Data: timeout_HLS, timeout_NLP
Result: kernel // with Merlin Pragma
nlp_file ← generate_nlp_file(kernel), min_lat ← ∞;
for max_array_partitioning ∈
{∞, 2048, 1024, 512, 256, 128, 64, 32, 16, 8, 1} do
  for parallelism ∈ {coarse + fine, fine} do
    current_nlp_file ←
      change_max_array_partitioning(copy(nlp_file),
        max_array_partitioning);
    if parallelism == fine then
      | add_constraint_only_fine_grained_parallelism(
        | current_nlp_file);
    end
    pragma_configuration, lower_bound ←
      SOLVER(current_nlp_file, timeout_NLP);
    if lower_bound < min_lat then
      | current_kernel ←
        | introduce_pragma(copy(kernel),
        | pragma_configuration);
      | hls_lat, valid ←
        | MERLIN(kernel, timeout_HLS);
      | if valid then // no over-utilization
        | | min_lat ← min(min_lat, hls_lat);
      | end
    end
  end
end

```

Algorithm 1: NLP-DSE

In order to reduce the maximum unroll factor and array partitioning, we modify the parameters specified in the NLP file. And we automatically add constraints (Eq 9) to restrict parallelism to fine-grained levels, as described in Section 5. The choice to restrict

the maximum array partitioning to the power of 2 is to improve the speed of the DSE. Adding possibilities would permit exploring a larger space and potentially finding a design with a faster latency at the cost of a longer DSE.

7 EVALUATION

We now present our experimental results using a set of polyhedral computation kernels.

7.1 Setup

We use kernels from Polybench/C 4.2.1 [20]. In addition we add a kernel of Convolution Neural Network (CNN). A single-precision floating point is utilized as the default data type in computations. Computations operate on medium and large datasets from PolyBench/C [20] in order to have kernels with large footprint and have a large enough space to explore. The problem size and loop order of CNN are $J,I=256, P,Q=5 H,W=224$. A description of each benchmark can be found in Table 2. The *ludcmp*, *deriche* and *nusinnov* kernels are not present as PolyOpt-HLS [22] does not handle negative loop stride. *Cholesky* and *correlation* contains a `sqrt()` operation which we do not support currently. Finally, we removed *FDTD-2D* because it exposed a bug in Merlin, and this generated a program where data dependencies are not fully preserved.

We evaluate designs with AMD/Xilinx Merlin [31]. The synthesis is carried out with AMD/Xilinx Vitis 2021.1. We choose the option "-funsafe-math-optimizations" to enable commutative/associative reduction operators and implementation of reductions in logarithmic time. We change the default on-chip memory size of Merlin by the size of the device we use. As the target hardware platform, we run the Xilinx Alveo U200 device where the target frequency is 250 MHz.

We analyze the kernels and automatically generate each NLP problem with a version of PolyOpt-HLS [21]. We modified and extended for our work. Employing the AMPL description language to solve the NLP problems, we ran the commercial BARON solver [23, 27] version 21.1.13. For our experiments, we utilize 2 Intel(R) Xeon(R) CPU E5-2680 v4 @ 2.40GHz and 252GB DDR4 memory.

7.2 Experimental Evaluation

We compare our method with AutoDSE [26], described in Section 2, and we automatically generate the space of AutoDSE with the command *ds_generator*. We replace the UF and tile size by all the UF and tile size which divide the TC in order to have the same space. AutoDSE doesn't impose any constraints on parallelism or the maximum array partitioning. It employs an incremental exploration approach, enabling it to make compiler-specific pragma selections.

Table 2 displays the space size of each design. The DSE is done in 4 parts with two threads for each (default parameter), with a timeout for the generation of the HLS report of 180 minutes, and a timeout of the DSE of 600 minutes (not always respected cf. Table 2). For our method we take the same parameters, and we add a timeout for BARON of 30 minutes.

7.3 Comparison with AutoDSE

Table 2 shows the comparison with AutoDSE. NL, ND, S, and Space S are respectively the number of loops, the number of polyhedral

dependencies (WaR, WaW, RaW), problem size (L for Large and M for Medium) and space size. For each method we compute the throughput (GF/s) in GFLOPs per second, the total time of the DSE (T) in minutes, the number of designs explored (DE) and the number of designs timeout (DT). In addition, for AutoDSE we add the number of design that are early rejected/prune (ER) as AutoDSE prunes the design when AMD/Xilinx Merlin can not apply one of the pragmas, due to its analysis limitations.

To illustrate the performance achievable *without a complete DSE*, the first synthesizable design found with NLP-DSE (FS) is displayed. Indeed, due to our under-estimation of resources, the theoretically best design produced by NLP solving may not be synthesizable. We report the improvements in DSE time (T) and throughput (GF/s).

The performance of the kernel evaluated show significant improvements in both time and throughput. The time of the DSE is 5.69x faster on average (3.70x for geo-mean) and the throughput is 17.24x higher on average (2.38x for geo-mean) for the kernel evaluated. For almost all (46/47) kernels and problem sizes the method identifies a design with a throughput similar to (+/- 2%), or better than, AutoDSE. We have a slight slowdown for *Doitgen* Large because NLP-DSE explores the design found by the NLP with a maximum array partitioning of 2048 which timeouts, and then 1024 which is the best design found. However AutoDSE finds a design with a maximum array partitioning of 1280. By changing the maximum array partitioning to 1280 we find the same configuration as AutoDSE. Thus it is possible to obtain designs with a better performance but at the cost of a longer search. For all kernels and problem sizes, except *Durbin*, NLP-DSE is faster than AutoDSE. AutoDSE prunes all configurations of *Durbin* which explains the speed of AutoDSE for this kernel.

We can observe a difference of the performance for the same kernel in function of the problem size. If we take the example of *2mm*, the difference has many factors. First as the footprint of the kernel becomes more important, it begins overusing the BRAMs. A large parallelism requires a bigger array partitioning which considerably increases the number of BRAMs and uses more BRAMs than available. Additionally, for large problems with high levels of parallelism, there are multiple instances of timeouts observed. Furthermore, the compilers applied the pragmas more efficiently for smaller problem sizes. We observe twice as many kernels where the pragmas are not applied as expected for the large problem size.

For *Atax* Large (Lst. 2), AutoDSE explores 166 designs of which 106 are early rejected and 30 timeout. AutoDSE starts by partially unrolling Loops 2 and 3 and will then attempt to do a coarse-grained parallelization on Loop 1 with all divisors, which is impossible due to dependencies. Although AutoDSE manages to prune/early reject the designs because Merlin cannot apply the pragmas, it still requires several minutes of compilation by Merlin for each unroll factor. In parallel, AutoDSE tries to pipeline the outermost loops (and therefore unroll the innermost loops) which creates numerous timeouts. Although the first two designs timeout due to too high level of parallelism, NLP-DSE allows us to find a configuration with the innermost loops unrolled with a UF=700. This allows us to find a design with a 3.46x higher throughput in 11.34x less time.

Our method experiences some timeouts for designs with high levels of parallelism. However, thanks to our DSE approach, we quickly identify optimized designs where each loop body has a

Kernel	NL	ND	S	Space S	FS	NLP-DSE				AutoDSE					Perf. Improvement	
					GF/s	GF/s	T	DE	DT	GF/s	T	DE	DT	ER	T	GF/s
covariance	7	34	M	1.80E+11	0.08	0.75	336	21	8	0.28	645	161	15	115	1.92x	2.64x
covariance	7	34	L	1.92E+13	0.39	0.73	466	21	9	0.62	2,849	209	68	118	6.11x	1.16x
2mm	6	13	M	1.37E+10	13.19	117.48	70	18	0	0.41	1,870	101	37	49	26.71x	288.88x
2mm	6	13	L	1.15E+12	0.57	2.17	456	17	3	0.40	1,835	291	38	240	4.02x	5.41x
3mm	9	19	M	1.20E+15	13.86	138.73	242	18	0	0.39	698	82	15	57	2.88x	354.12x
3mm	9	19	L	6.18E+17	0.18	1.01	486	19	3	0.59	968	112	18	81	1.99x	1.71x
atax	4	12	M	1.40E+05	1.96	1.96	194	10	1	1.98	1,653	175	13	136	8.52x	0.99x
atax	4	12	L	1.60E+07	0.47	1.52	205	11	2	0.44	2,325	166	30	106	11.34x	3.46x
bicg	3	10	M	1.90E+04	0.99	0.99	248	12	1	0.98	729	65	2	28	2.94x	1.01x
bicg	3	10	L	4.44E+05	1.68	1.68	218	12	1	0.50	3,355	236	42	176	15.39x	3.38x
cnv	6	2	-	6.43E+06	0.39	97.99	213	16	1	97.99	1,292	28	19	480	6.06x	1.00x
doitgen	5	30	M	8.64E+06	19.75	19.75	193	13	0	18.95	819	296	14	248	4.24x	1.04x
doitgen	5	30	L	3.63E+07	0.08	102.62	241	20	1	110.66	1,299	222	24	169	5.39x	0.93x
durbin	4	55	M	1.08E+02	0.01	0.20	193	7	4	0.12	134	25	0	23	0.69x	1.65x
durbin	4	55	L	9.00E+00	0.12	0.12	212	3	1	0.12	31	7	0	5	0.15x	1.00x
gemm	4	6	M	2.30E+06	105.18	105.18	185	21	1	68.91	1,345	86	27	34	7.27x	1.53x
gemm	4	6	L	1.47E+07	32.98	32.98	450	18	7	2.77	2,810	188	47	133	6.24x	11.89x
gemver	7	13	M	7.72E+11	0.78	9.45	218	21	4	2.99	847	65	5	28	3.89x	3.16x
gemver	7	13	L	1.28E+13	9.94	9.94	290	21	7	0.18	1,756	221	206	10	6.06x	54.69x
gesummv	2	17	M	6.12E+02	1.97	1.97	220	14	3	1.97	836	80	8	47	3.80x	1.00x
gesummv	2	17	L	6.33E+03	1.82	2.64	236	18	1	0.56	692	94	29	60	2.93x	4.73x
gramschmidt	6	34	M	1.75E+07	1.58	1.58	364	7	3	0.44	934	109	92	8	2.57x	3.56x
gramschmidt	6	34	L	1.22E+08	2.34	2.34	420	6	4	0.95	819	265	11	239	1.95x	2.47x
lu	5	16	M	2.28E+03	0.03	0.03	614	19	11	0.04	849	193	1	159	1.38x	0.98x
lu	5	16	L	3.99E+03	0.03	0.04	335	9	2	0.03	812	258	5	219	2.42x	1.03x
mvt	4	6	M	1.38E+07	7.77	7.77	212	17	1	7.77	893	166	6	106	4.21x	1.00x
mvt	4	6	L	7.41E+07	12.90	12.90	181	20	3	1.10	1,240	249	20	189	6.85x	11.78x
symm	3	33	M	2.31E+04	0.04	0.20	63	5	0	0.20	691	142	35	89	10.97x	1.00x
symm	3	33	L	6.64E+04	0.21	0.31	540	8	5	0.21	612	731	0	692	1.13x	1.52x
syr2k	4	6	M	2.32E+04	0.07	1.74	224	16	2	1.20	685	230	17	203	3.06x	1.45x
syr2k	4	6	L	6.67E+04	1.30	1.42	420	15	7	1.30	768	293	21	262	1.83x	1.09x
syrk	4	6	M	2.32E+04	0.49	1.32	224	16	2	0.61	631	280	4	264	2.82x	2.15x
syrk	4	6	L	6.67E+04	0.94	2.07	466	17	7	0.65	643	410	0	398	1.38x	3.16x
trisolv	2	13	M	3.60E+02	0.03	0.03	69	12	0	0.04	694	69	33	23	10.06x	0.98x
trisolv	2	13	L	6.30E+02	0.04	0.04	75	18	0	0.04	651	127	2	98	8.68x	0.99x
trmm	3	8	M	2.31E+04	0.01	0.05	20	16	0	0.04	630	401	4	367	31.50x	1.29x
trmm	3	8	L	6.64E+04	0.02	0.06	425	17	2	0.03	760	167	159	4	1.79x	1.79x
floyd-warshall	3	21	M	8.65E+04	0.17	0.61	246	17	3	0.10	1,605	60	22	29	6.52x	6.15x
floyd-warshall	3	21	L	3.29E+06	0.17	1.31	381	20	6	0.10	2,728	150	71	77	7.16x	13.09x
heat-3d	7	42	M	3.04E+07	0.23	3.75	402	17	7	3.75	928	75	33	35	2.31x	1.00x
heat-3d	7	42	L	4.37E+07	0.13	0.62	520	13	6	0.63	740	109	70	35	1.42x	0.99x
jacobi-1d	3	14	M	1.48E+03	11.43	11.43	55	4	0	11.53	948	126	3	74	17.24x	0.99x
jacobi-1d	3	14	L	4.00E+04	5.95	5.95	386	9	6	2.65	1,283	173	21	123	3.32x	2.25x
jacobi-2d	5	22	M	8.07E+06	0.20	3.32	379	12	5	3.32	674	158	26	98	1.78x	1.00x
jacobi-2d	5	22	L	1.14E+07	0.26	1.25	427	9	6	1.25	1,106	231	39	171	2.59x	1.00x
seidel-2d	3	27	M	4.26E+03	0.05	0.05	365	5	1	0.05	796	103	27	68	2.18x	1.01x
seidel-2d	3	27	L	1.77E+05	0.05	0.05	540	13	7	0.05	880	91	33	48	1.63x	1.00x
Average					5.38	15.11	296			7.44	1,123				5.69x	17.24x
Geo. Mean					0.51	1.54	247			0.65	916				3.70x	2.38x

Table 2: Comparison with AutoDSE

similar level of parallelism. For 20/47 cases, the first synthesizable design is equal to the best design of the DSE. This is because compilers can be conservative and not apply pragmas as expected. In

this case, another configuration is applied than what was identified by the NLP, which explains the difference in performance.

7.4 Accuracy

The tightness of the lower bound estimation relies on the correct application of pragma directives such as pipeline and parallel. It also assumes that Merlin can efficiently transfer memory from off-chip to on-chip using 512-bit chunks. Finally, it assumes that Merlin optimally handles the transfer of memory from off-chip to on-chip. Figures 1a and 1b compare the measured HLS latency for every synthesizable design explored during our DSE with its predicted latency per solving the NLP. The Y-axis represents $\log(\text{latency})$ and the X-axis the rank of the design sorted by HLS latency. For Fig 1b we exclude designs when we detect that the pragma parallel and pipeline are not applied as defined by Merlin. We observe that about half of the designs have at least one pragma not applied, leading logically to a larger difference between measured and predicted latency. Generally speaking, for parallelization pragmas, Merlin is more restrictive for coarse-grained parallelization, in many cases these pragmas are not applied. We also observe certain cases where the partitioning is not done correctly which does not allow a pipeline with $\Pi=1$ when it is theoretically possible. For Figure 1b we observe a better overall accuracy, albeit imperfect. These differences are due in large part to how Merlin eventually implemented memory transfers, which we model optimistically.

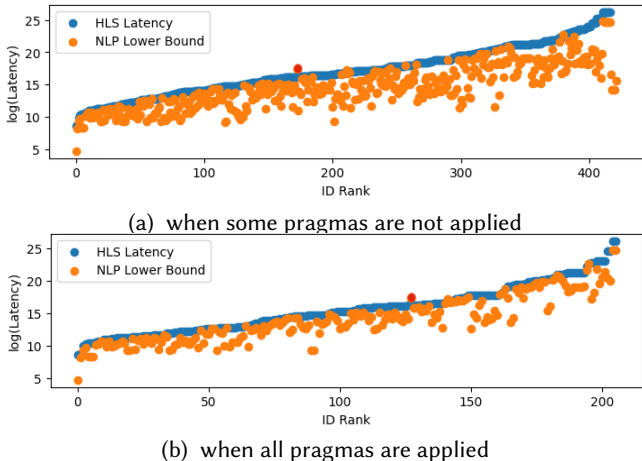


Figure 1: Comparison of the HLS Latency vs. Lower Bound

We observe in Fig. 1a and Fig. 1b one configuration where the lower bound property is not maintained (shown in red). This corresponds to a configuration of the Heat-3d kernel, where the pragma `loop_flatten` has been applied automatically, which changes the program structure. Overall unless Vitis applies `loop_flatten` automatically, which we do not model, our estimate is a lower bound for the cases evaluated.

7.5 Scalability

To mitigate prolonged solving times for specific kernels and problem sizes, we’ve implemented a 30-minute timeout constraint for the BARON solver. While this timeout doesn’t guarantee achieving optimality, it ensures that the solver provides the best solution it has found within the time limit. In Table 3, we present statistics regarding the number of problem timeouts (ND T/O) and problem non-timeouts (ND NT/O), along with the average time in seconds (Avg Time) for all problems and exclusively for those that did not

time out. We can note that the 20 NLP problems for CNN finish in few seconds with an average of 3.71 seconds.

We notice that 12 kernels exhibit at least one NLP problem that times out. To investigate scalability further, we conducted restarts for NLP problems that timed out at 30 minutes, extending the timeout to 30 hours. For 30 out of 126 problems (23.8%), we found an optimal theoretical solution within an average time of 3.13 hours. We observe that problems timing out after 30 hours often involve trip counts with numerous divisors, significantly expanding the space for the unroll factor. Consequently, non-linear conditions involving more than three unknown variables of unroll factors (UFs) become extremely time-consuming to resolve. By relaxing these constraints, we are able to find a solution in seconds but this can result in infeasible designs due to over-utilization of resources as these constraints are removed. For 23.8% of problems not timing out at 30 hours, we examined the disparity in objective function values provided by the solver when it times out at 30 minutes (representing the best solution found so far) versus when it discovers the optimal solution. For 25 out of 30 problems, the estimated latency is exactly the same. However, for the remaining 5 problems, the differences in the estimated latencies range from a mere 0.04% up to 2,426%.

Size	ND T/O	ND NT/O	Avg Time	Avg Time NT/O
Medium	7	469	55s	29s
Large	119	361	479s	43s
All	126	830	268s	35s

Table 3: Study of the scalability

8 RELATED WORK

NLP-DSE makes it possible to automatically introduce pragmas in order to obtain a design with a good QoR. Many previous works using different DSE methods have the same objective. Model-free DSEs [10, 26, 34] evaluate each candidate by generating the HLS report. The synthesis time or report generation can last several hours, which considerably reduces the explored design space. Additionally, some DSE, such as [26], may lead to local minima. In order to avoid the synthesis time limitation, model-based DSEs and AI-driven DSEs have been developed. They estimate the performance of each design using a cost model [1, 29, 29, 37–40], Graph Neural Networks (GNN) [25, 30] or decision trees [17, 19, 35]. These DSEs estimate the QoR of the design in a few milliseconds. However, the evaluation of a large number of designs can still take several hours and the accuracy may not match the HLS report. Hence, evaluating only the top- n results with HLS may lead to sub-optimal solutions. Other works allow one-shot optimization with code transformations, e.g., [33] but the space of hardware directives and code transformations is limited. Some focus on a predefined micro-architectures, e.g., [28] but are limited in their application. NLP-DSE is a hybrid approach: our cost model in the form of NLP makes it possible to consider very large design spaces in a few minutes. This makes it potentially even faster than existing cost models. Yet we rely on HLS to ensure accurate performance.

Recent advances in optimization solvers such as BARON [23, 27] have allowed NLP-based approaches to become a promising alternative to approximate ILP-based methods, as they can encode more complex and realistic performance models. Previous works [2, 21, 41] encode a cost model as Linear Programming (LP) problem.

However, it requires an approximation, such as approximating the volume of communication inter loops [2, 21], or simplifying the space by exposing direct parallelization in the problem [41].

The selection of tile sizes remains fundamental for the final QoR. Similar to our approach, [16] uses a cost model to select the tile size. Although their space is much more complete than ours as we are restricted to Merlin's transformations, their method does not allow the evaluation of the whole space.

9 CONCLUSION

Our work targets the automatic selection of pragma configurations for HLS with a framework that automatically inserts Merlin pragmas into loop-based programs. Our framework is guided by an analytical performance and resource model, which serves as a lower bound estimation for the achievable performance across all possible configurations.

REFERENCES

- [1] André Bannwart Perina, Jürgen Becker, and Vanderlei Bonato. 2019. Lina: Timing-Constrained High-Level Synthesis Performance Estimator for Fast DSE. In *2019 International Conference on Field-Programmable Technology (ICFPT)*. 343–346. <https://doi.org/10.1109/ICFPT47387.2019.00063>
- [2] Uday Bondhugula, Albert Hartono, J. Ramanujam, and P. Sadayappan. 2008. A Practical Automatic Polyhedral Parallelizer and Locality Optimizer. In *Proceedings of the 29th ACM SIGPLAN Conference on Programming Language Design and Implementation* (Tucson, AZ, USA) (*PLDI '08*). Association for Computing Machinery, New York, NY, USA, 101–113. <https://doi.org/10.1145/1375581.1375595>
- [3] Jason Cong, Muhuan Huang, Peichen Pan, Yuxin Wang, and Peng Zhang. 2016. Source-to-Source Optimization for HLS. In *FPGAs for Software Programmers*, Dirk Koch, Frank Hannig, and Daniel Ziener (Eds.). Springer, 137–163. <http://dblp.uni-trier.de/db/books/collections/KHZ2016.html#CongHPW016>
- [4] Jason Cong, Muhuan Huang, Peichen Pan, Di Wu, and Peng Zhang. 2016. Software Infrastructure for Enabling FPGA-Based Accelerations in Data Centers: Invited Paper. In *Proceedings of the 2016 International Symposium on Low Power Electronics and Design* (San Francisco Airport, CA, USA) (*ISLPED '16*). Association for Computing Machinery, New York, NY, USA, 154–155. <https://doi.org/10.1145/2934583.2953984>
- [5] Jason Cong, Bin Liu, Stephen Neuendorffer, Juanjo Noguera, Kees Visser, and Zhiru Zhang. 2011. High-Level Synthesis for FPGAs: From Prototyping to Deployment. *IEEE Transactions on Computer-Aided Design of Integrated Circuits and Systems* 30, 4 (2011), 473–491. <https://doi.org/10.1109/TCAD.2011.2110592>
- [6] Venmugil Elango, Fabrice Rastello, Louis-Noël Pouchet, Jagannathan Ramanujam, and Ponnuswamy Sadayappan. 2015. On characterizing the data access complexity of programs. In *Proceedings of the 42nd Annual ACM SIGPLAN-SIGACT Symposium on Principles of Programming Languages*.
- [7] P. Feautrier. 1988. Parametric integer programming. *RAIRO-Rech. Oper.* 22, 3 (1988), 243–268.
- [8] Paul Feautrier. 1991. Dataflow analysis of array and scalar references. *International Journal of Parallel Programming* 20, 1 (1991), 23–53.
- [9] P. Feautrier. 1992. Some efficient solutions to the affine scheduling problem, part II: multidimensional time. *International Journal of Parallel Programming* 21, 6 (1992), 389–420.
- [10] Lorenzo Ferretti, Giovanni Ansaloni, and Laura Pozzi. 2018. Lattice-Traversing Design Space Exploration for High Level Synthesis. In *2018 IEEE 36th International Conference on Computer Design (ICCD)*. 210–217. <https://doi.org/10.1109/ICCD.2018.00040>
- [11] Sylvain Girbal, Nicolas Vasilache, Cédric Bastoul, Albert Cohen, David Parello, Marc Sigler, and Olivier Temam. 2006. Semi-Automatic Composition of Loop Transformations. *International Journal of Parallel Programming* 34, 3 (June 2006), 261–317.
- [12] Sitao Huang, Kun Wu, Hyunmin Jeong, Chengyue Wang, Deming Chen, and Wen-Mei Hwu. 2021. PyLog: An Algorithm-Centric Python-Based FPGA Programming and Synthesis Flow. *IEEE Trans. Comput.* 70, 12 (2021), 2015–2028. <https://doi.org/10.1109/TC.2021.3123465>
- [13] Intel. 2023. Intel. <https://www.intel.com/content/www/us/en/software/programmable/quartus-prime/hls-compiler.html>
- [14] Yi-Hsiang Lai, Yuze Chi, Yuwei Hu, Jie Wang, Cody Hao Yu, Yuan Zhou, Jason Cong, and Zhiru Zhang. 2019. HeteroCL: A Multi-Paradigm Programming Infrastructure for Software-Defined Reconfigurable Computing. In *Proceedings of the 2019 ACM/SIGDA International Symposium on Field-Programmable Gate Arrays* (Seaside, CA, USA) (*FPGA '19*). Association for Computing Machinery, New York, NY, USA, 242–251. <https://doi.org/10.1145/3289602.3293910>
- [15] Jiajie Li, Yuze Chi, and Jason Cong. 2020. HeteroHalide: From Image Processing DSL to Efficient FPGA Acceleration. In *Proceedings of the 2020 ACM/SIGDA International Symposium on Field-Programmable Gate Arrays* (Seaside, CA, USA) (*FPGA '20*). Association for Computing Machinery, New York, NY, USA, 51–57. <https://doi.org/10.1145/3373087.3375320>
- [16] Junyi Liu, John Wickerson, and George A. Constantinides. 2017. Tile size selection for optimized memory reuse in high-level synthesis. In *2017 27th International Conference on Field Programmable Logic and Applications (FPL)*. 1–8. <https://doi.org/10.23919/FPL.2017.8056810>
- [17] H. Mohammadi Makrani, F. Farahmand, H. Sayadi, S. Bondi, S. Pudukotai Dinakararao, H. Homayoun, and S. Rafatirad. 2019. Pyramid: Machine Learning Framework to Estimate the Optimal Timing and Resource Usage of a High-Level Synthesis Design. In *2019 29th International Conference on Field Programmable Logic and Applications (FPL)*. IEEE Computer Society, Los Alamitos, CA, USA, 397–403. <https://doi.org/10.1109/FPL.2019.00069>
- [18] Microchip. 2023. SmartHLS Compiler Software. <https://www.microchip.com/en-us/products/fpgas-and-plds/fpga-and-soc-design-tools/smarthls-compiler>
- [19] Kenneth O'Neal, Mitch Liu, Hans Tang, Amin Kalantar, Kennen DeRenard, and Philip Brisk. 2018. HLSPredict: Cross Platform Performance Prediction for FPGA High-Level Synthesis. In *2018 IEEE/ACM International Conference on Computer-Aided Design (ICCAD)*. 1–8. <https://doi.org/10.1145/3240765.3240816>
- [20] PolyBench [n. d.]. *PolyBench/C 4.2.1*. <http://polybench.sourceforge.net>
- [21] Louis-Noël Pouchet, Peng Zhang, P. Sadayappan, and Jason Cong. 2013. Polyhedral-Based Data Reuse Optimization for Configurable Computing. In *Proceedings of the ACM/SIGDA International Symposium on Field Programmable Gate Arrays* (Monterey, California, USA) (*FPGA '13*). Association for Computing Machinery, New York, NY, USA, 29–38. <https://doi.org/10.1145/2435264.2435273>
- [22] Louis-Noël Pouchet, Peng Zhang, P. Sadayappan, and Jason Cong. 2013. Polyhedral-Based Data Reuse Optimization for Configurable Computing. In *21st ACM/SIGDA International Symposium on Field-Programmable Gate Arrays (FPGA'13)*. ACM Press, Monterey, California.
- [23] N. V. Sahinidis. 2017. *BARON 21.1.13: Global Optimization of Mixed-Integer Nonlinear Programs*, User's Manual.
- [24] Siemens. 2023. Catapult High-Level Synthesis. <https://eda.sw.siemens.com/en-US/ic/catapult-high-level-synthesis/>
- [25] Atefeh Sohrabzadeh, Yunsheng Bai, Yizhou Sun, and Jason Cong. 2022. Automated Accelerator Optimization Aided by Graph Neural Networks. In *2022 59th ACM/IEEE Design Automation Conference (DAC)*.
- [26] Atefeh Sohrabzadeh, Cody Hao Yu, Min Gao, and Jason Cong. 2021. AutoDSE: Enabling Software Programmers Design Efficient FPGA Accelerators. In *The 2021 ACM/SIGDA International Symposium on Field-Programmable Gate Arrays* (Virtual Event, USA) (*FPGA '21*). Association for Computing Machinery, New York, NY, USA, 147. <https://doi.org/10.1145/3431920.3439464>
- [27] M. Tawarmalani and N. V. Sahinidis. 2005. A polyhedral branch-and-cut approach to global optimization. *Mathematical Programming* 103 (2005), 225–249. Issue 2.
- [28] Jie Wang, Licheng Guo, and Jason Cong. 2021. AutoSA: A Polyhedral Compiler for High-Performance Systolic Arrays on FPGA. In *The 2021 ACM/SIGDA International Symposium on Field-Programmable Gate Arrays* (Virtual Event, USA) (*FPGA '21*). Association for Computing Machinery, New York, NY, USA, 93–104. <https://doi.org/10.1145/3431920.3439292>
- [29] Shuo Wang, Yun Liang, and Wei Zhang. 2017. FlexCL: An analytical performance model for OpenCL workloads on flexible FPGAs. In *2017 54th ACM/EDAC/IEEE Design Automation Conference (DAC)*. 1–6. <https://doi.org/10.1145/3061639.3062251>
- [30] Nan Wu, Yuan Xie, and Cong Hao. 2023. IronMan-Pro: Multiobjective Design Space Exploration in HLS via Reinforcement Learning and Graph Neural Network-Based Modeling. *IEEE Transactions on Computer-Aided Design of Integrated Circuits and Systems* 42, 3 (2023), 900–913. <https://doi.org/10.1109/TCAD.2022.3185540>
- [31] AMD Xilinx. 2023. Merlin. <https://github.com/Xilinx/merlin-compiler>
- [32] AMD Xilinx. 2023. Vitis. <https://www.xilinx.com/products/design-tools/vitis/vitis-platform.html>
- [33] Hanchen Ye, HyeGang Jun, Hyunmin Jeong, Stephen Neuendorffer, and Deming Chen. 2022. ScaleHLS: A Scalable High-Level Synthesis Framework with Multi-Level Transformations and Optimizations: Invited. In *Proceedings of the 59th ACM/IEEE Design Automation Conference* (San Francisco, California) (*DAC '22*). Association for Computing Machinery, New York, NY, USA, 1355–1358. <https://doi.org/10.1145/3489517.3530631>
- [34] Cody Hao Yu, Peng Wei, Max Grossman, Peng Zhang, Vivek Sarker, and Jason Cong. 2018. S2FA: An Accelerator Automation Framework for Heterogeneous Computing in Datacenters. In *2018 55th ACM/ESDA/IEEE Design Automation Conference (DAC)*. 1–6. <https://doi.org/10.1109/DAC.2018.8465827>
- [35] Mang Yu, Sitao Huang, and Deming Chen. 2021. Chimera: A Hybrid Machine Learning-Driven Multi-Objective Design Space Exploration Tool for FPGA High-Level Synthesis. In *Intelligent Data Engineering and Automated Learning - IDEAL 2021*, Huijun Yin, David Camacho, Peter Tino, Richard Allmendinger, Antonio J. Tallón-Ballesteros, Ke Tang, Sung-Bae Cho, Paulo Novais, and Susana Nascimento (Eds.). Springer International Publishing, Cham, 524–536.
- [36] Zhiru Zhang, Yiping Fan, Wei Jiang, Guoling Han, Changqi Yang, and Jason Cong. 2008. *AutoPilot: A Platform-Based ESL Synthesis System*. Springer Netherlands, Dordrecht, 99–112. https://doi.org/10.1007/978-1-4020-8588-8_6
- [37] Jieru Zhao, Liang Feng, Sharad Sinha, Wei Zhang, Yun Liang, and Bingsheng He. 2017. COMBA: A comprehensive model-based analysis framework for high level synthesis of real applications. In *2017 IEEE/ACM International Conference on Computer-Aided Design (ICCAD)*. 430–437. <https://doi.org/10.1109/ICCAD.2017.8203809>
- [38] Guanwen Zhong, Alok Prakash, Yun Liang, Tulika Mitra, and Smail Niar. 2016. Lin-Analyzer: A high-level performance analysis tool for FPGA-based accelerators. In *2016 53rd ACM/EDAC/IEEE Design Automation Conference (DAC)*. 1–6. <https://doi.org/10.1145/2897937.2898040>
- [39] Guanwen Zhong, Alok Prakash, Siqi Wang, Yun Liang, Tulika Mitra, and Smail Niar. 2017. Design Space exploration of FPGA-based accelerators with multi-level parallelism. In *Design, Automation Test in Europe Conference Exhibition (DATE), 2017*. 1141–1146. <https://doi.org/10.23919/DATE.2017.7927161>
- [40] Wei Zuo, Warren Kemmerer, Jong Bin Lim, Louis-Noël Pouchet, Andrey Ayupov, Taemin Kim, Kyungtae Han, and Deming Chen. 2015. A polyhedral-based SystemC modeling and generation framework for effective low-power design space exploration. In *2015 IEEE/ACM International Conference on Computer-Aided Design (ICCAD)*. 357–364. <https://doi.org/10.1109/ICCAD.2015.7372592>

- [41] Wei Zuo, Louis-Noel Pouchet, Andrey Ayupov, Taemin Kim, Chung-Wei Lin, Shinichi Shiraishi, and Deming Chen. 2017. Accurate High-Level Modeling and Automated Hardware/Software Co-Design for Effective SoC Design Space Exploration. In *Proceedings of the 54th Annual Design Automation Conference 2017* (Austin, TX, USA) (*DAC '17*). Association for Computing Machinery, New York, NY, USA, Article 78, 6 pages. <https://doi.org/10.1145/3061639.3062195>

We present in this appendix more details about key elements of our analytical performance model, and the associated proofs this model computes a lower bound on latency under resource constraints. Note we plan to publish this appendix on ArXiv if our paper is accepted.

.1 Analytical Model Template

Let $I_i^{\vec{P}V_i}(X)$ the operators defined as follows:

$$I_i^{\vec{P}V_i}(X) = [II_i * (TC_i^{avg}/uf_i - ispipelined_i)] \odot X$$

where \odot is $+$ if $ispipelined_i = 1$, $*$ otherwise. We also have:

$$C_i^{\vec{P}V_i}(X_1, X_2, \dots, X_n) = \max(X_1, X_2, \dots, X_n) \text{ if } inparallel_i$$

and

$$C_i^{\vec{P}V_i}(X_1, X_2, \dots, X_n) = \sum_{k=1}^n X_k \text{ if } insequence_i$$

with $inparallel_i = 1 - insequence_i$ if (X_1, X_2, \dots, X_n) do not

have dependencies (WaR, RaW, WaW) else 0. Finally, $SL_i^{\vec{P}V_i}(\vec{S}_k)$ denotes a region of straight-line code (e.g., an inner-loop body). Intuitively, SL will represent a lower bound on the latency of a code block such that by composition across all loops as per the template formula, the result remains a lower bound on the full program latency.

Given the summary AST of the program in constructor form, and the set of $\vec{P}V_i$ vectors for each loop, we build the analytical formula template as follows: (1) replace the $Loop_i(\vec{X})$ operator by $I_i^{\vec{P}V_i}(\vec{X})$ operator; (2) replace the \vec{X} list by $C_i^{\vec{P}V_i}(\vec{X})$; and (3) replace statement lists inside loop i \vec{S}_x by $SL_i^{\vec{P}V_i}(\vec{S}_x)$. That is for our example, we simply rewrite: $Loop_i(Loop_{j_1}(S1), Loop_{j_2}(S2, S3))$ into $I_i^{\vec{P}V_i}(C_i^{\vec{P}V_i}(I_{j_1}^{\vec{P}V_{j_1}}(SL_{j_1}^{\vec{P}V_{j_1}}(S1)), I_{j_2}^{\vec{P}V_{j_2}}(SL_{j_2}^{\vec{P}V_{j_2}}(S2, S3))))$

.2 A Formal Model for Latency

Our objective is to formulate a lower bound on the latency of a program after HLS. We therefore have put several restrictions: we assume the input program is a polyhedral program, that is the control-flow is statically analyzable; all loops can be recognized and their trip count computed; and all array / memory accesses can be exactly modeled at compile-time. No conditional can occur in the program. While our approach may generalize beyond this class, we limit here to these strict assumptions.

To maintain a lower bound on latency by composition, we operate on a representation of (parts of the) program which is both schedule-independent and storage-independent: indeed, a lower bound on this representation is necessarily valid under any schedule and storage eventually implemented. *We however require HLS to not change the count and type of operations.* Furthermore, for lower bounding purposes, we assume unless stated otherwise $\forall i$, $inparallel_i = 1$. We will discuss in the next section a more realistic but compiler-dependent approach to set $inparallel_i$, based on dependence analysis.

We assume programs are made of affine loops, that are loops with statically computable control-flow, with loop bounds made only of intersection of affine expressions of surrounding loop iterators and program constants. We now assume loop bodies (i.e., statements surrounded by loops) have been translated to a list of

statements, with at most a single operation (e.g., $+$, $-$, $/$, $*$) per statement. Operations are n-ary, that is they take $n \geq 0$ input scalar values as operand, and produce 0 or 1 output scalar value. A memory location can be loaded from (resp. stored to) an address stored in a scalar variable. This is often referred to as straight-line code. This normalization of the loop body facilitates the computation of live-in/live-out data for the code block, and the extraction of the computation graph. Note the region can be represented in Static Single Assignment form, to ensure different storage location for every assignment, facilitating the construction of the operation graph. In addition we suppose that the input program don't have useless operation i.e., there is no dead-code elimination as in the Listing 3.

```

1 int example(int y, int z){
2   int x;
3   x = 12 + y; // dead-code elimination
4   x = y + z;
5   return x;
6 }

```

Listing 3: Example with dead code elimination

The restriction can be summarized as:

- The input program is a pure polyhedral program [11], and its analysis (loop trip counts for every loop, all data dependencies [8]) is exact.
- No HLS optimization shall change the number of operations in the computation: strength reduction, common sub-expression elimination, etc. shall either first be performed in the input program before analysis, or not be performed by the HLS toolchain.
- The program does not contain "useless" operations. A typical case is when a value is overwritten before being used.
- We only model DSP and BRAM resources for the considered kernel, ignoring all other resources.
- We assume resource (DSP) sharing across different operations executing at the same cycle is not possible.

Definition .1 (Straight-line code). An n-ary operation takes n scalar operands \vec{i} as input, and produces a single scalar o as output. A statement contains a single n-ary operation, or a load from (resp. store to) a memory location to (resp. from) a scalar. A straight-line code region L is a list of consecutive statements, with a single entry and single exit.

Definition .2 (Live-in set). The live-in set V_I^L of region L is the set of scalar values, variables and memory locations that read before being written, under any possible valid execution of L .

Definition .3 (Live-out set). The live-out set V_O^L of region L is the set of variables and memory locations that written to during any possible valid execution of L .

We can compute the directed acyclic graph made of all statements (i.e., all n-ary operations), connecting all producer and consumer operations, to build the operation graph:

Definition .4 (Operation Graph). Given a straight-line code region R made of a list L of statements $S \in L$, the operation graph OG is the directed graph $\langle \{N, V_I, root, V_O\}, E \rangle$ such that $\forall S_i \in L, N_{S_i} \in N$;

and for every operation with output o and inputs \vec{i} in $L \forall S_i, \forall i_k \in \vec{i}_{S_i}, e_{i_k, o} \in E, \forall S_i : (o_{S_i}, \vec{i}_{S_i}) \in L, S_j : (o_{S_j}, \vec{i}_{S_j}) \in L$ with $S_i \neq S_j$ then we have $E_{S_i, S_j} \in E$ iff $o_{S_i} \cap \vec{i}_{S_j} \neq \emptyset$. For every input (resp. output) in S_i which is not matched with an output (resp. input) of another S_j in L , create a node $V_{oal} \in V_I$ (resp. V_O) for this input (resp. output) value. If $\dim(\vec{i}_{S_i}) = 0$ then an edge e_{root, S_i} is added to E .

From this representation, we can easily define key properties to subsequently estimate the latency and area of this code region, such as its span, or critical path.

Definition .5 (Operation Graph critical path). Given OG^L an operation graph for region L . Its critical path OG_{cp} is the longest of all the shortest paths between every pairs $(v_i, v_o) \in \langle \{V_I, root\}, V_O \rangle$. Its length is noted $\#OG_{cp}^L$.

.2.1 Estimating Latency. We can build a simple a lower bound on the latency of an operation graph:

THEOREM .6 (LOWER BOUND ON LATENCY OF AN OPERATION GRAPH). *Given infinite resources, and assuming no operation nor memory movement can take less than one cycle to complete, the latency $LAT_{cp}^L \geq \#OG_{cp}^L$ is a lower bound on the minimal feasible latency to execute L .*

PROOF TH .6. Every operation S_i is associated at least one edge with a source in $\langle \{V_I, root\} \rangle$, so there is a path between one of these nodes and every operation by construction in Def. .4. For an operation to produce a useful output, there must be a path from its output to a node in V_O , otherwise the operation may be removed by dead code elimination. Therefore the shortest path sp between a pair of node $(v_i, v_o) \in \langle \{V_I, root\}, V_O \rangle$ is the shortest sequence of operations in dependence that must be executed to produce v_o . As any operation takes at least one cycle to complete per Def. .6, then this path must take at least $\#sp$ cycles to complete. As we take the largest of shortest paths between all possible pairs (v_i, v_o) then OG_{cp}^L is the length of the longest shortest path to produce any output v_o from some input, via a sequence of producer-consumer operations. Therefore it must take at least $\#OG_{cp}^L$ cycles to execute this path. \square

We can then build a tighter lower bound on the number of cycles a region L may take to execute, under fixed resources, by simply taking the maximum between the weighted span and the work to execute normalized by the resources available.

THEOREM .7 (LATENCY LOWER BOUND UNDER OPERATION RESOURCE CONSTRAINTS). *Given R_{op} a count of available resources of type op , for each operation type, and $LO(op)$ the latency function for operation op , with $LO(op) \geq 1$. $\#L(op)$ denotes the number of operations of type op in L . We define $LO(\#OG_{cp}^L) = \sum_{n \in cp} LO(n)$ the critical path weighted by latency of its operations. The minimal latency of a region L is bounded by*

$$Lat_{R_{op}}^L \geq \max(LO(\#OG_{cp}^L), \max_{o \in op} (\#L(o) \times LO(o) / R_o))$$

PROOF TH .7. Suppose $\forall o \in op, R_o \geq \#L(o)$. Then there is equal or more resources available than work to execute, this is equivalent

to the infinite resource hypothesis of Th. .6, the minimal latency is $LO(\#OG_{cp}^L)$.

Suppose $\exists o \in op, R_o < \#L(o)$. Then there exists at least one unit in R_o that is executing $\lceil \#L(o) / R_o \rceil$ operations. As every operation op takes at $L(op) \geq 1$ cycle to complete, this unit will execute in at least $\lceil \#L(o) \times L_o / R_o \rceil$ cycles. If $\lceil \#L(o) \times L_o / R_o \rceil \geq LO(\#OG_{cp}^L)$, the computation cannot execute in less than $\lceil \#L(o) \times L_o / R_o \rceil$ cycles. \square

.2.2 Loop Unrolling: full unroll. We start by reasoning on the bound for latency of a loop nest which has been fully unrolled, e.g. as a result of `#pragma ACCEL parallel` or `#pragma HLS unroll`. Full unrolling amounts to fully unroll all TC iterations of a loop, replacing the loop by TC replications of its original loop body, where the loop iterator has been updated with the value it takes, for each replication.

It follows a simple corollary:

COROLLARY .8 (EQUIVALENCE BETWEEN FULLY UNROLLED AND STRAIGHT-LINE CODE). *Given a loop nest l , if full unrolling is applied to l then the code obtained after full unrolling is a straight-line code as per Def. .1.*

PROOF Co .8. By construction the process of fully unrolling all the loops creates a straight-line code region without loop control, which therefore fits Def. .1. \square

Consequently, we can bound the latency of a fully unrolled loop nest:

THEOREM .9 (MINIMAL LATENCY OF A FULLY UNROLLED LOOP NEST). *Given a loop nest l , which is first rewritten by fully unrolling all loops to create a straight-line code region L . Given available resources R_{op} and latencies $L(op) \geq 1$. Then its minimal latency is bounded by:*

$$Lat_{R_{op}}^L \geq \max(LO(\#OG_{cp}^L), \max_{o \in op} (\lceil \#L(o) \times L_o / R_o \rceil))$$

PROOF TH .9. By Corollary .8. \square

.2.3 Loop Unrolling: partial unroll. Loop unrolling is a HLS optimization that aims to execute multiple iterations of a loop in parallel. Intuitively, for an unroll factor $UF \geq 1$, UF replications of the loop body will be instantiated. If $TC_l \bmod UF_l \neq 0$ then an epilogue code to execute the remaining $TC_l \bmod UF_l$ iterations is needed.

Partial unrolling can be viewed as a two-step transformation: first strip-mine the loop by the unroll factor, then consider the inner loop obtained is fully-unrolled. The latency of the resulting sub-program is determined by how the outer-loop generated will be implemented. We assume without additional explicit information this outer loop will execute in a non-pipelined, non-parallel fashion, to provide the following bound:

THEOREM .10 (MINIMAL LATENCY OF A PARTIALLY UNROLLED LOOP WITH FACTOR UF). *Given a loop l with trip count TC_l and loop body L , and unroll factor $UF \leq TC$. Given available resources R_{op} and latencies $L(op) \geq 1$. Given L' the loop body obtained by replicating UF times the original loop body L . Then the minimal latency of l if executed in a non-pipelined fashion is bounded by:*

$$Lat_{R_{op}}^{L, S} \geq \lceil TC / UF \rceil \times Lat_{R_{op}}^{L'}$$

PROOF TH .10. By construction and Theorem .7, $Lat_{R_{op}}^{L'}$ is a lower bound on the latency of L' , that is the sub-program made of UF iterations of the loop. $\lfloor TC/UF \rfloor \leq TC_1/UF$ is a lower bound on the number of iterations of the loop. As we assume a non-pipelined execution for the resulting outer loop, every iteration shall start after the completion of the preceding one, that is its iteration latency, itself bounded by $Lat_{R_{op}}^{L'}$. \square

Note this bound requires to build the operation graph for the whole loop body. This is straightforward for inner loops and/or fully unrolled loop nests, but impractical if the loop body contains other loops. We therefore define a weaker, but more practical, bound:

THEOREM .11 (MINIMAL LATENCY OF A PARTIALLY UNROLLED LOOP WITH FACTOR UF AND COMPLEX LOOP BODIES). *Given a loop l with trip count TC_1 and loop body L , and unroll factor $UF \leq TC$. Given available resources R_{op} and latencies $L(op) \geq 1$. Then the minimal latency of l if executed in a non-pipelined fashion is bounded by:*

$$Lat_{R_{op}}^{L,S} \geq \lfloor TC/UF \rfloor * Lat_{R_{op}}^L$$

PROOF TH .11. Given OG^i and OG^j two CDAGs, for a pair of distinct iterations i, j of loop l .

If $V_O^i \cap V_O^j = \emptyset$, then the graph $OG^{i,j}$ made of the two iterations i, j cannot have a smaller critical path length than OG^i and OG^j : there is no edge crossing OG^i and OG^j in $OG^{i,j}$ since outputs are distincts, therefore $Lat(OG^{i,j}) \geq \max(Lat(OG^i), Lat(OG^j))$.

If $V_O^i \cap V_O^j \neq \emptyset$. Then iterations i and j produce at least one output in common. As there is no useless operation, the graph $OG^{i,j}$ made of the two iterations i, j can not be smaller than OG^i or OG^j and hence $Lat(OG^{i,j}) \geq \max(Lat(OG^i), Lat(OG^j))$. \square

Vitis allows to do a reduction with a tree reduction in logarithmic time with the option "unsafe-math".

THEOREM .12 (MINIMAL LATENCY OF A PARTIALLY UNROLLED LOOP WITH FACTOR UF FOR REDUCTION LOOP WITH TREE REDUCTION). *Given a reduction loop l with trip count TC_1 and loop body L , and unroll factor $UF \leq TC$. Given available resources R_{op} and latencies $L(op) \geq 1$. Then the minimal latency of l , if executed in a non-pipelined fashion and the tree reduction is legal is bounded by:*

$$Lat_{R_{op}}^{L,S} \geq \lfloor TC/UF \rfloor \times Lat_{R_{op}}^L \times \lceil \log_2(UF) \rceil$$

PROOF TH .12. By definition a reduction loop is a loop with a dependency distance of 1. Hence, at each iteration the same memory cell is read and write. Because of the dependency distance of 1, only one element can be add to the same memory cell. However each data can be add independently two by two and the result of this independent addition can also be add two by two until we obtained one value. Hence the reduction can be done in $\log_2(UF)$ iterations with a tree reduction. As the depth of the tree is $\log_2(UF)$ and each node at the same depth can be execute independently in $Lat_{R_{op}}^L$ cycles the straight line code has a latency greater or equal to $Lat_{R_{op}}^L \times \lceil \log_2(UF) \rceil$. And then similarly to Th. .11 and .12 the sequential execution of the loops without pragma repeat this process $\lfloor TC/UF \rfloor$ times.

.2.4 *Loop pipelining.* Loop pipelining amounts to overlapping multiple iterations of the loop, so that the next iteration can start prior to the completion of the preceding one. The initiation interval (II) measures in cycles the delay between the start of two consecutive iterations. \square

It follows a bound on the minimal latency of a pipelined loop:

THEOREM .13 (MINIMAL LATENCY OF A PIPELINED LOOP WITH KNOWN II). *Given a loop l with trip count TC_1 and loop body L . Given available resources R_{op} and latencies $L(op) \geq 1$. Then the minimal latency of l if executed in a pipelined fashion is bounded by:*

$$Lat_{R_{op}}^{L,P} \geq Lat_{R_{op}}^L + II * (TC_1 - 1)$$

PROOF TH .13. $Lat_{R_{op}}^L$ is the minimal latency to complete one iteration of l by Theorem .7. The initiation interval measures the number of elapsed cycles before the next iteration can start, it takes therefore at least $TC_1 * II - 1$ to start $TC_1 - 1$ iterations, irrespective of their completion time. Therefore the latency of the loop is at least the latency of one iteration to complete, and for all iterations to be started. \square

.2.5 *Non-Parallel, Non-Pipelined Loops.* We conclude by a trivial case: if the loop is not optimized by any directive (including any automatically inserted by the compilers), that is is not parallelized nor pipelined, then every next iteration of the loop starts only after the end of the prior iteration.

Definition .14 (Lower bound on latency of a non-parallel, non-pipelined loop under resources constraints). *Given a loop l with trip count TC_1 which is neither pipelined nor parallelized, that is, iteration $i + 1$ starts after the full completion of iteration i , for all iterations. Given $Lat_{R_{op}}^L$ the minimal latency of its loop body. Then*

$$Lat_{R_{op}}^L \geq TC_1 * Lat_{R_{op}}^L$$

.2.6 *Program latency lower bound.* We now focus on having the program latency lower bound, with resource constraints. This bound takes into account the limitations imposed by available resources, which can significantly affect the achievable performance. We assume here that the resources consumed are only consumed by the computing units and resource use by the computational unit of one operation can not be reused by the computational unit of another operation executing at the same time. We also assume that the compilers have implemented the pragma configuration given as input.

For DSPs we suppose we have a perfect reuse i.e., that the computation units for the same operation can be reused as soon as the computation unit is not in use. Under-estimating the resources used is fundamental to proving the latency lower bound, as otherwise another design that consumes less resource than predicted may be feasible, itself possibly leading to a better latency.

THEOREM .15. *Given a loop body L , the set of statements \mathcal{S} , $\#L_{op}^s$ the number of operation op for the statements s , DSP_{op} the number of resource (DSPs) used for the operation op , MCU_{op}^s the maximal computational unit the statement s can use in parallel and the configuration of pragma which is constitute of the vectors $\vec{P}\vec{V}_i$ for each loop.*

The minimal number of resource (DSPs) consumed, R_{used}^{min} , by L for the pragma configuration is the sum, for each operation, of the maximum number of DSPs used in parallel by a statement. This correspond to:

$$R_{used}^{min} = \sum_{op} \max_{s \in S} (\#L_{op}^s \times DSP_{op} \times MCU_{op}^s)$$

PROOF TH .15. Considering perfect resource reuse, where all unused computational units can be reused, and assuming that the compilers have implemented the pragma configuration provided as input. For each statement s , the maximum number of computational units used in parallel is determined. This means that each statement s requires at least $\#L_{op}^s \times DSP_{op} \times MCU_{op}^s$ DSPs. By considering the maximum across all statements, we can guarantee that at least one statement will require $\max_{s \in S} (\#L_{op}^s \times DSP_{op} \times MCU_{op}^s)$ DSPs. Since there is no possibility of resource reuse between different operations, the summation of the resource consumed for each operation remains the minimum consumption of resources. In other words, the sum of the individual resource consumption for each operation represents the minimum amount of resources required. \square

The lower bound of a kernel is therefore the lower bound of the configuration such that the minimal resource consumption is less than or equal to the resource available.

THEOREM .16 (COMPUTATION LOWER BOUND OF THE KERNEL UNDER RESOURCE CONSTRAINT). Given a loop body L , the set of statements S , $\#L_{op}^s$ the number of operation op for the statements s , DSP_{op} the number of resources (DSPs) used for the operation op , MCU_{op}^s the maximal computational unit the statement s can use in parallel and the configuration of pragma which is constitute of the vectors $\vec{P}\vec{V}_i$ for each loop.

The configuration of pragma, which has the minimal lower bound and which respect $R_{used}^{min} = \sum_{op} \max_{s \in S} (\#L_{op}^s \times DSP_{op} \times MCU_{op}^s) \leq R_{op}$, is the lower bound of the kernel.

PROOF TH .16. According to Theorem .15, R_{used}^{min} is the minimal number of DSP a configuration can use. Hence, all configuration which does not respect the constraint $R_{used}^{min} \leq R_{op}$ have a over-utilization of the resource and hence are invalid.

Hence, the minimal lower bound of each configuration of pragma is the lower bound of the kernel. \square

.2.7 *Memory transfer.* AMD/Xilinx Merlin manages automatically the memory transfer. The memory transfer and computation are not overlap (no dataflow) hence the latency is the sum of the latency of computation and communication. We assume that for each array the contents of the array are in the same DRAM bank.

THEOREM .17 (LOWER BOUND OF THE MEMORY LATENCY FOR AN ARRAY). Given a loop body L , the set of array \mathcal{A} , an array $a \in \mathcal{A}$, and LAT_a^{mem} the latency to transfer the array a from off-chip to on-chip (inputs) and from on-chip to off-chip (outputs). $\forall a \in \mathcal{A}, LAT_a^{mem} \geq (\mathbb{1}_{a \in V_O^L} + \mathbb{1}_{a \in V_I^L}) \times footprint_a / max_burst_size$. With $\mathbb{1}_{cond} = 1$ if $cond = true$ else 0.

PROOF TH .17. In order to transfer all the element of the array a we can use packing with a maximum packing allowed by the target

device of max_burst_size , which mean in practice the real burst size will be equal or less than max_burst_size . As all the elements of the array a are in the same bank the transfer is sequential. And as we suppose all operation including memory transfer are done in at least one cycle the minimum latency is $footprint_a / max_burst_size$ to transfer one time the array a . As an array can be input, output or both we need to add the transfer from off-chip to on-chip for inputs i.e. $a \in V_I^L$ and from on-chip to off-chip for the outputs i.e. $a \in V_O^L$. \square

THEOREM .18 (LOWER BOUND OF THE MEMORY LATENCY). Given a loop body L , the set of array \mathcal{A} , the number of cycle to transfer the array a is bounded by $\max_{a \in \mathcal{A}} (\mathbb{1}_{a \in V_O^L} + \mathbb{1}_{a \in V_I^L}) \times footprint_a / max_burst_size$.

PROOF TH .18. According to Th. .17 the lower bound to transfer one array a is $(\mathbb{1}_{a \in V_O^L} + \mathbb{1}_{a \in V_I^L}) \times footprint_a / max_burst_size$. As the array can be on different DRAM banks the transfer from off-chip to on-chip can be done in parallel but at least one array have a latency greater or equal to $(\mathbb{1}_{a \in V_O^L} + \mathbb{1}_{a \in V_I^L}) \times footprint_a / max_burst_size$ and hence the memory latency is equal to $\max_{a \in \mathcal{A}} (\mathbb{1}_{a \in V_O^L} + \mathbb{1}_{a \in V_I^L}) \times footprint_a / burst_size$. \square

.2.8 *Summary.* We have the lower bound of the computation and communication. As the computation and communication are not overlap the lower bound of a kernel is the sum of lower bound of the computation for this kernel and of the lower bound for the communication for this kernel. This can be summarize with the theorem .19

THEOREM .19 (LOWER BOUND OF THE KERNEL). Given a loop body L , the set of statements S , the set of array \mathcal{A} , $\#L_{op}^s$ the number of operation op for the statements s , DSP_{op} the number of resources (DSPs) used for the operation op , MCU_{op}^s the maximal computational unit the statement s can use in parallel and the configuration of pragma which is constitute of the vectors $\vec{P}\vec{V}_i$ for each loop.

The configuration of pragma, which has a sum of the minimal lower bound of computation and communication and which respect $R_{used}^{min} = \sum_{op} \max_{s \in S} (\#L_{op}^s \times DSP_{op} \times MCU_{op}^s) \leq R_{op}$, is the lower bound of the kernel.